

Parameterizing Dark Energy Models and Study of Finite Time Future Singularities

Tanwi Bandyopadhyay^{1*} and Ujjal Debnath^{2†}

¹*Department of Mathematics, Adani Institute of Infrastructure Engineering, Ahmedabad-382421, Gujarat, India.*

²*Department of Mathematics, Indian Institute of Engineering Science and Technology, Shibpur, Howrah-711103, India.*

A review on spatially flat D-dimensional Friedmann-Robertson-Walker (FRW) model of the universe has been performed. Some standard parameterizations of the equation of state parameter of the Dark Energy models are proposed and the possibilities of finite time future singularities are investigated. It is found that certain types of these singularities may appear by tuning some parameters appropriately. Moreover, for a scalar field theoretic description of the model, it was found that the model undergoes bouncing solutions in some favorable cases.

Keywords: Future Singularity, Dynamical Dark Energy, Scalar Field, Parameterizations.

PACS numbers: 04.50.Kd

I. INTRODUCTION

In order to avoid the initial singularity problem [1], a competitive alternative structure is proposed to the standard inflationary description. This is called the big bounce scenario ([2]-[10]). In this framework, the universe initially contracts continuously up to an initial narrow state with a non-zero minimal radius and then transforms to an expanding phase [11]. This means that the initial singularity is replaced by a bounce and consequently the cosmic equation of state (EoS) parameter crosses the phantom divide line (from $\omega < -1$ to $\omega > -1$).

On the other hand, various cosmological observations indicate the current cosmic acceleration ([12]-[21]). To explain this phenomenon in the homogeneous and isotropic universe, it is necessary to assume a component of matter with large negative pressure, called dark energy. Since the inception of this concept, a wide variety of phenomenological models have been proposed as the most suitable candidate of dark energy. Among them, the cosmological constant provides plausible answers but suffers from the fine-tuning problem. This issue has forced researchers to probe models having time-dependent equation of state parameter for the dark energy component. A simple classification of these models could be as follows:

1. Cosmological constant ($\omega \equiv \frac{p}{\rho} = -1$)
2. Dark energy with $\omega = \text{constant} \neq -1$ [cosmic strings ($\omega = -\frac{1}{3}$), domain walls ($\omega = -\frac{2}{3}$)].
3. Dynamical dark energy ($\omega = \omega(z) \neq \text{constant}$) (i.e., quintessence, Chaplygin gas, k-essence, braneworld) ([22]-[30])
4. Dark energy with $\omega(z) < -1$ [scalar-tensor theory, phantom models] ([31],[32])

The reconstruction problem for dark energy is reviewed in [33] in much detail (see also the references therein). Recently, in the literature [34], the possibilities of future singularities have been studied in the framework of Modified Chaplygin Gas filled universe and conditions of bounce were investigated. In this work, we provide more general results in terms of the possibilities of finite time future singularities in the context of a D-dimensional Friedmann-Robertson-Walker universe by imposing five standard parameterizations of the dark energy equation of state parameter. Different aspects of dark energy models have been studied so far to reconcile standard cosmological scenario with observations but no work has been done to the parameterization of these models in view of investigating the finite time future singularities.

* tanwi.bandyopadhyay@aiim.ac.in

† ujjaldebnath@gmail.com, ujjal@associates.iucaa.in

The paper is organized as follows. In section II, we state the governing equations of the metric in the D -dimensional Universe. In section III, the description for the major physical quantities are provided in the backdrop of five different parameterization models both analytically and graphically. In section IV, the possibilities of future singularities are examined for these five models and the possible restrictions for certain type of singularity are shown in tabular form. In Section V, the bouncing universe is described in the five parameterization model and finally, we end with a short discussion in section VI.

II. D-DIMENSIONAL FRIEDMANN-ROBERTSON-WALKER UNIVERSE

We consider the D -dimensional spatially flat Friedmann-Robertson-Walker universe, given by [34]

$$ds^2 = -dt^2 + a^2(t)d\Omega^2 \quad (1)$$

where $a(t)$ is the scale factor and $d\Omega^2$ is the metric for the $(D - 1)$ dimensional space. The field equations together with the energy conservation equation can be obtained as (assuming $8\pi G = c = 1$)

$$H^2 = \frac{2\rho}{(D-1)(D-2)} \quad (2)$$

$$\dot{H} + H^2 = -\frac{(D-1)p + (D-3)\rho}{(D-1)(D-2)} \quad (3)$$

and

$$\dot{\rho} + (D-1)H(\rho + p) = 0 \quad (4)$$

Here $H = \frac{\dot{a}}{a}$ denotes the Hubble parameter. In the following section and subsequent sub-sections, we will examine different parameterizations of dark energy models and attain analytical as well as graphical expressions of some physical entities involved in the process.

III. DARK ENERGY AS SCALAR FIELD FOR VARIOUS PARAMETERIZATION MODELS

By considering scalar field ϕ with the potential $U(\phi)$, the effective Lagrangian [34] is given by

$$L_\phi = \frac{\dot{\phi}^2}{2} - U \quad (5)$$

So the energy density and pressure take the form

$$\rho = \frac{\dot{\phi}^2}{2} + U \quad (6)$$

$$p = \frac{\dot{\phi}^2}{2} - U \quad (7)$$

The kinetic energy for the field is given by

$$\dot{\phi}^2 = (1 + \omega)\rho \quad (8)$$

where $\omega = \frac{p}{\rho}$. One can always write $\dot{\phi} = \phi'z$, where the prime denotes differentiation with respect to redshift $z = \frac{1}{1+a}$. With the help of (2), we have

$$\phi' = \sqrt{\frac{(D-1)(D-2)(1+\omega)}{2}} \frac{1}{1+z} \quad (9)$$

The scalar potential associated with the field is given by

$$U = \frac{1}{2}(1-\omega)\rho \quad (10)$$

In the next subsections, we will investigate the scalar field and its potential in different well known parameterization models. A detailed review of different dark energy models can be found in [35].

A. Model I : Linear Parameterization

Here we assume the linear equation of state [36] $\omega = \omega(z) = \omega_0 + \omega_1 z$. Here ω_0 and ω_1 are constants. Using equation (4), the energy density of the model then gives rise to

$$\rho = \rho_0(1+z)^{(D-1)(1+\omega_0-\omega_1)} e^{(D-1)\omega_1 z} \quad (11)$$

Here ρ_0 is the present value of the energy density. The pressure of the fluid then becomes

$$p = (\omega_0 + \omega_1 z)\rho_0(1+z)^{(D-1)(1+\omega_0-\omega_1)} e^{(D-1)\omega_1 z} \quad (12)$$

Then (9) reduce to

$$\phi' = \sqrt{\frac{(D-1)(D-2)}{2}} \frac{\sqrt{1+\omega_0+\omega_1 z}}{1+z} \quad (13)$$

which on further integration gives rise to the scalar field as

$$\phi = \phi_0 + \sqrt{2(D-1)(D-2)} \left[\sqrt{1+\omega_0+\omega_1 z} - M \tan^{-1} \left(\frac{\sqrt{1+\omega_0+\omega_1 z}}{M} \right) \right] \quad (14)$$

where $M = \sqrt{\omega_1 - \omega_0 - 1}$. Also (10) changes to

$$U = \frac{1}{2}(1-\omega_0-\omega_1 z)\rho_0(1+z)^{(D-1)(1+\omega_0-\omega_1)} e^{(D-1)\omega_1 z} \quad (15)$$

We draw the variations of energy density ρ , pressure p , EoS parameter $\omega(z)$, Hubble parameter H , potential $U(\phi)$ and the scalar field ϕ with the variation in z in Figs. 1 - 6 respectively. Fig. 7 shows the variation of $U(\phi)$ with ϕ . We observe that ρ , H and ϕ decrease as z decreases. p and ω decrease from positive level to negative level as z decreases. $U(\phi)$ first increases up to certain value of z and then decreases as z decreases. Also $U(\phi)$ decreases as ϕ increases.

B. Model II : Chevallier-Polarski-Linder (CPL) Parameterization

In the Chevallier-Polarski-Linder (CPL) Parameterization model, the equation of state is given by [37, 38] $\omega = \omega(z) = \omega_0 + \omega_1 \frac{z}{1+z}$. Here again ω_0 and ω_1 are constants. With these, the expressions of energy density, pressure, scalar field and the potential become

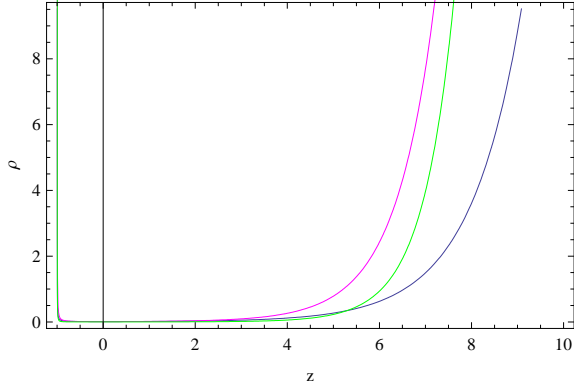


Fig.1

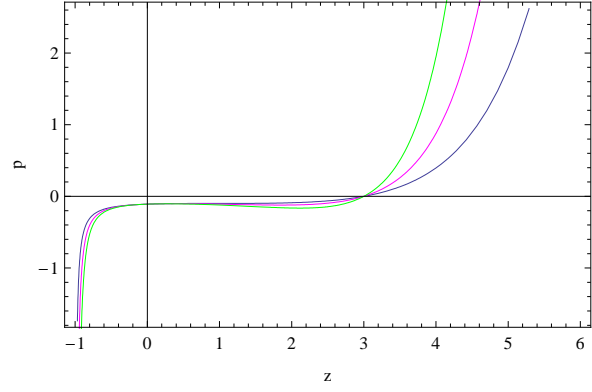


Fig.2

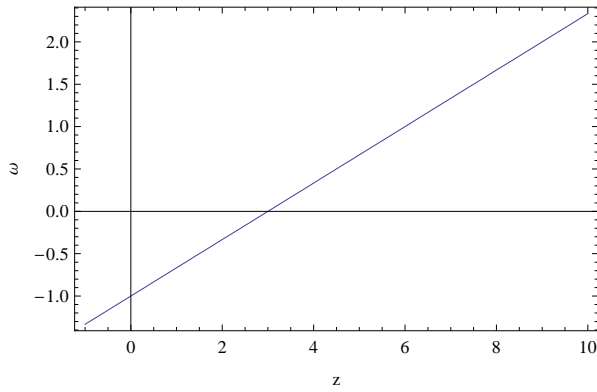


Fig.3

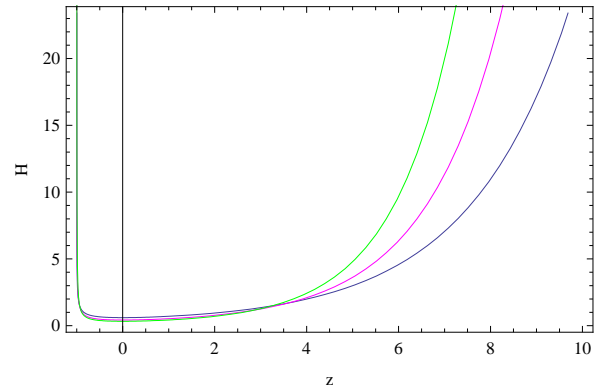


Fig.4

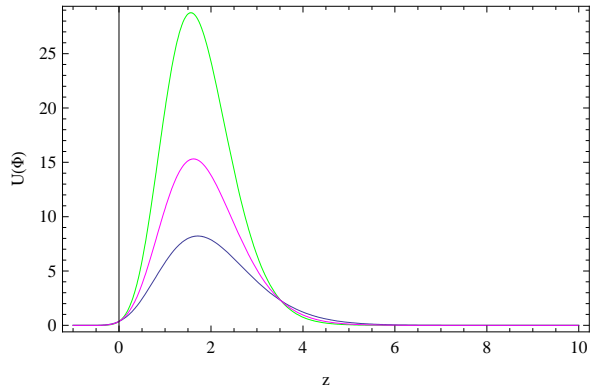


Fig.5

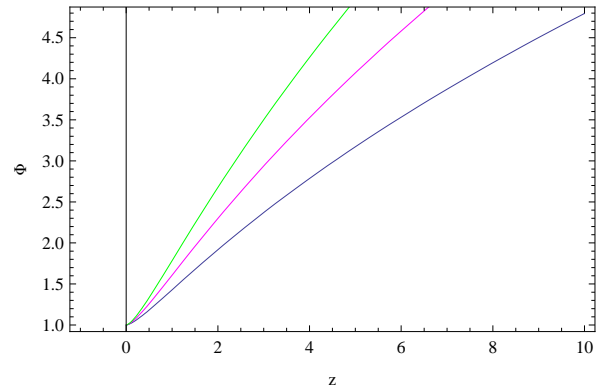


Fig.6

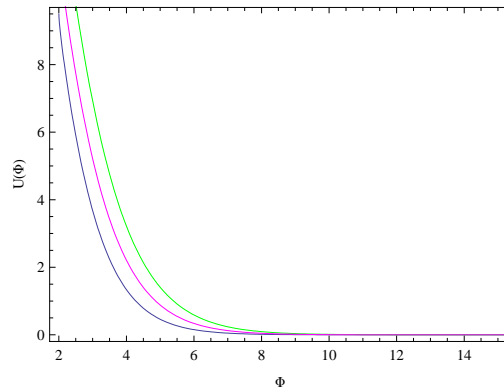


Fig.7

Figs. 1, 2, 3, 4, 5 and 6 show the variation of energy density ρ , pressure p , EoS parameter $\omega(z)$, Hubble parameter H , potential $U(\phi)$ and the scalar field ϕ with the variation in z for the **Linear** parameterizations. Fig. 7 shows the variation of $U(\phi)$ with ϕ . Different colored paths are obtained for different values of D .

$$\rho = \rho_0(1+z)^{(D-1)(1+\omega_0+\omega_1)} e^{-\frac{(D-1)\omega_1 z}{1+z}} \quad (16)$$

$$p = \left(\omega_0 + \omega_1 \frac{z}{1+z} \right) \rho_0(1+z)^{(D-1)(1+\omega_0+\omega_1)} e^{-\frac{(D-1)\omega_1 z}{1+z}} \quad (17)$$

$$\begin{aligned} \phi = \phi_0 + \sqrt{2(D-1)(D-2)} & \left[\sqrt{1+\omega_0+\omega_1} \log \left\{ (1+\omega_0+\omega_1)\sqrt{1+z} \right. \right. \\ & \left. \left. + \sqrt{1+\omega_0+\omega_1} \sqrt{(1+\omega_0)(1+z)+\omega_1 z} \right\} - \sqrt{(1+\omega_0) + \frac{\omega_1 z}{1+z}} \right] \end{aligned} \quad (18)$$

and

$$U = \frac{1}{2} \left(1 - \omega_0 - \omega_1 \frac{z}{1+z} \right) \rho_0(1+z)^{(D-1)(1+\omega_0+\omega_1)} e^{-\frac{(D-1)\omega_1 z}{1+z}} \quad (19)$$

We draw the variations of energy density ρ , pressure p , EoS parameter $\omega(z)$, Hubble parameter H , potential $U(\phi)$ and the scalar field ϕ with the variation in z in Figs. 8 - 13 respectively. Fig. 14 shows the variation of $U(\phi)$ with ϕ . We observe that ρ , H , and $U(\phi)$ first decrease up to $z = 0$ as z decreases and then sharply increase as z decreases. But p first increases up to $z = 0$ as z decreases and then sharply decreases as z decreases but keeps the negative level. ω decrease as z decreases and always keeps negative sign. ϕ increases as z decreases. Also $U(\phi)$ decreases as ϕ increases.

C. Model III : Jassal-Bagla-Padmanabhan (JBP) Parameterization

For the Jassal-Bagla-Padmanabhan (JBP) Parameterization model, the equation of state changes to [39] $\omega = \omega(z) = \omega_0 + \omega_1 \frac{z}{(1+z)^2}$, where ω_0 and ω_1 are constants. The following expressions are subsequently obtained as

$$\rho = \rho_0(1+z)^{(D-1)(1+\omega_0)} e^{\frac{(D-1)\omega_1 z^2}{2(1+z)^2}} \quad (20)$$

$$p = \left[\omega_0 + \omega_1 \frac{z}{(1+z)^2} \right] \rho_0(1+z)^{(D-1)(1+\omega_0)} e^{\frac{(D-1)\omega_1 z^2}{2(1+z)^2}} \quad (21)$$

$$\begin{aligned} \phi = \phi_0 + \sqrt{\frac{(D-1)(D-2)}{2}} & \left[-\sqrt{1+\omega_0 + \frac{\omega_1 z}{(1+z)^2}} + \frac{\sqrt{\omega_1}}{2} \tan^{-1} \left\{ \frac{\sqrt{\omega_1}(z-1)}{\sqrt{\omega_1 z + (1+\omega_0)(1+z)^2}} \right\} \right. \\ & \left. + \sqrt{1+\omega_0} \text{Log} \left\{ \omega_1 + 2(1+\omega_0)(1+z) + 2\sqrt{1+\omega_0} \sqrt{\omega_1 z + (1+\omega_0)(1+z)^2} \right\} \right] \end{aligned} \quad (22)$$

$$U = \frac{1}{2} \left[1 - \omega_0 - \omega_1 \frac{z}{(1+z)^2} \right] \rho_0(1+z)^{(D-1)(1+\omega_0)} e^{\frac{(D-1)\omega_1 z^2}{2(1+z)^2}} \quad (23)$$

We draw the variations of energy density ρ , pressure p , EoS parameter $\omega(z)$, Hubble parameter H , potential $U(\phi)$ and the scalar field ϕ with the variation in z in Figs. 15 - 20 respectively. Fig. 21 shows the variation of $U(\phi)$ with ϕ . We observe that ρ , H , and $U(\phi)$ first decrease up to $z = 0$ as z decreases and then sharply increase as z decreases. But p first increases up to $z = 0$ as z decreases and then sharply decreases as z decreases but keeps the negative level. ω first increases up to certain value of z and then sharply decreases but keeps negative sign. ϕ decreases as z decreases. Also $U(\phi)$ increases as ϕ increases.

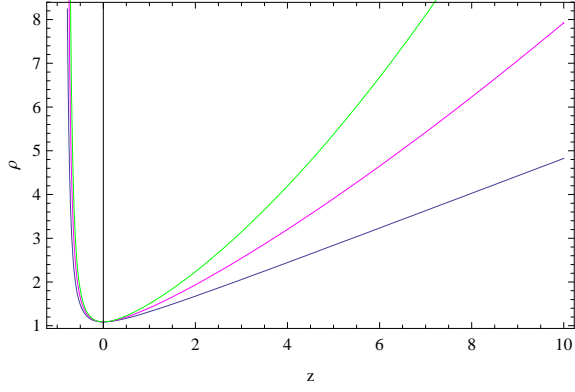


Fig.8

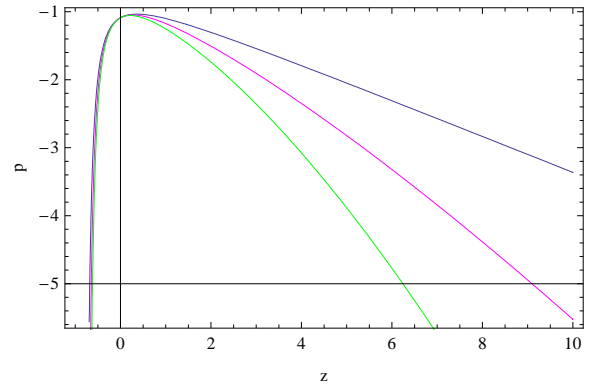


Fig.9

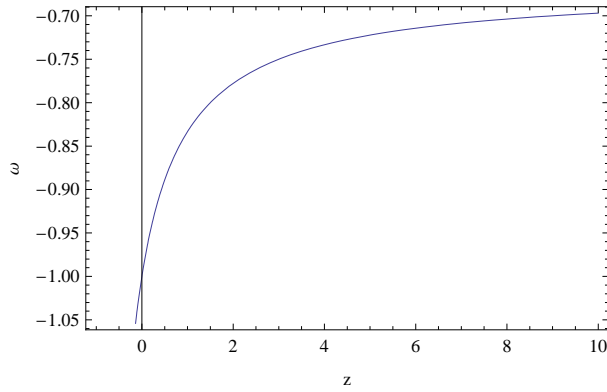


Fig.10

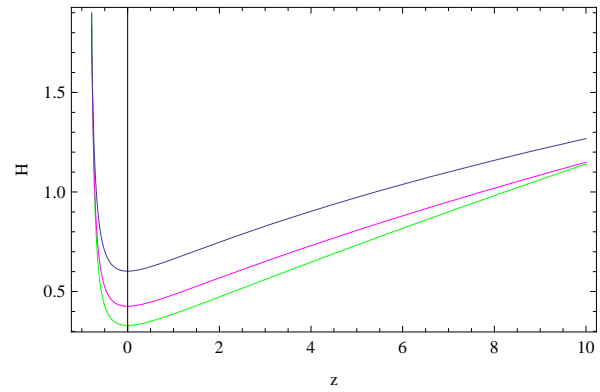


Fig.11

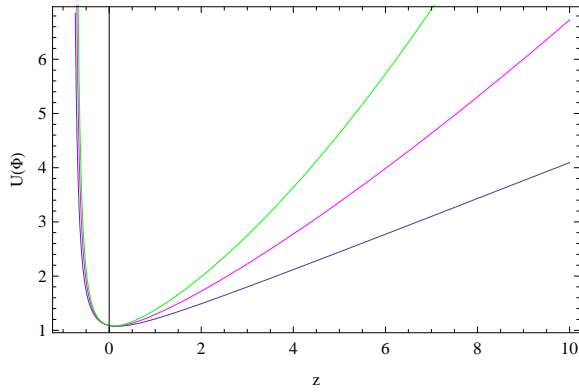


Fig.12

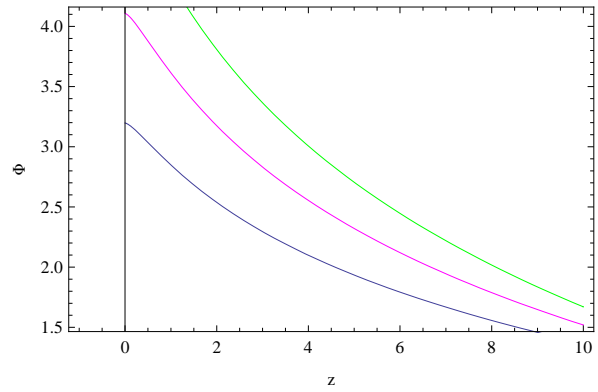


Fig.13

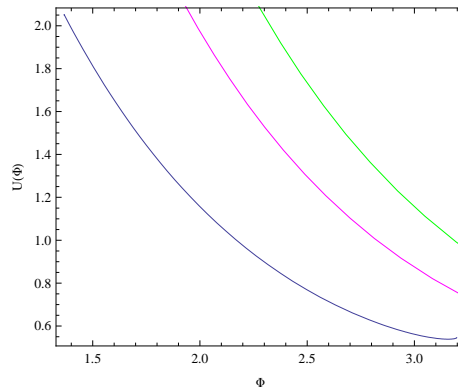


Fig.14

Figs. 8, 9, 10, 11, 12 and 13 show the variation of energy density ρ , pressure p , EoS parameter $\omega(z)$, Hubble parameter H , potential $U(\phi)$ and the scalar field ϕ with the variation in z for the CPL parameterizations. Fig. 14 shows the variation of $U(\phi)$ with ϕ . Different colored paths are obtained for different values of D .

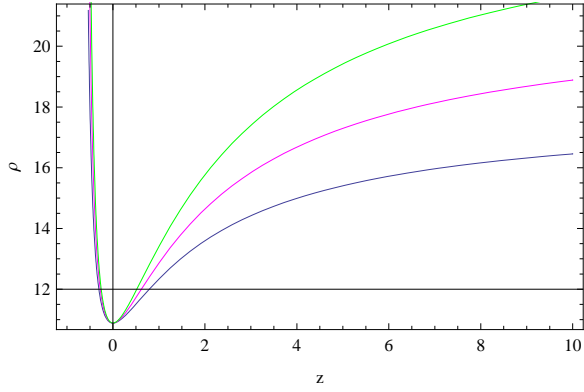


Fig.15

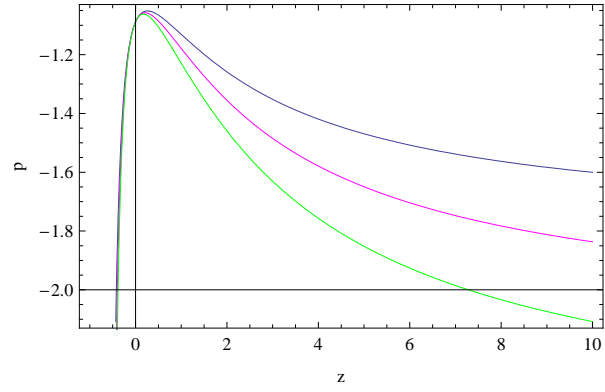


Fig.16

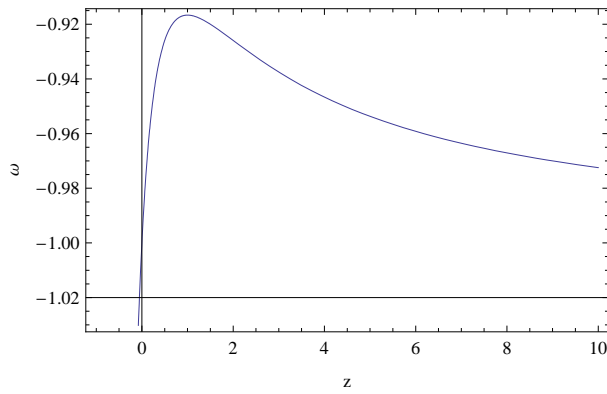


Fig.17

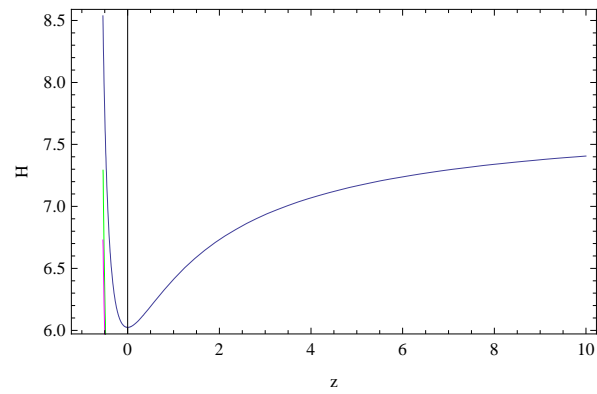


Fig.18

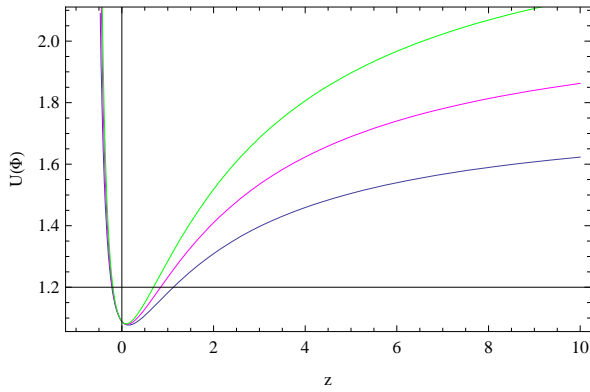


Fig.19

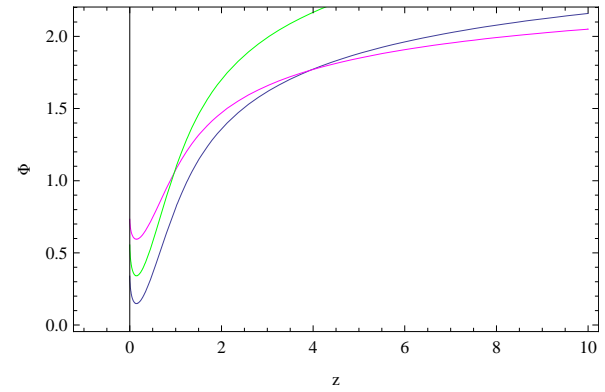


Fig.20

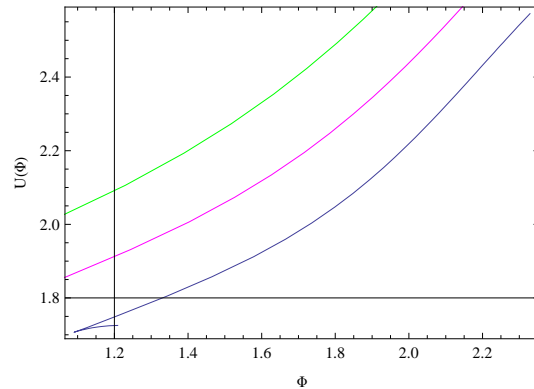


Fig.21

Figs. 15, 16, 17, 18, 19 and 20 show the variation of energy density ρ , pressure p , EoS parameter $\omega(z)$, Hubble parameter H , potential $U(\phi)$ and the scalar field ϕ with the variation in z for the **JBP** parameterizations. Fig. 21 shows the variation of $U(\phi)$ with ϕ . Different colored paths are obtained for different values of D .

D. Model IV: Alam-Sahni-Saini-Starobinsky (ASSS) Parameterization

In the Alam-Sahni-Saini-Starobinsky (ASSS) parameterization model, the equation of state parameter has the expression [40, 41]

$$\omega = \omega(z) = -1 + \frac{A_1(1+z) + 2A_2(1+z)^2}{3[A_0 + A_1(1+z) + A_2(1+z)^2]} \quad (24)$$

where, A_0 , A_1 and A_2 are constants. In this case, the physical parameters ρ , p , ϕ and U become

$$\rho = \rho_0 \left[\frac{A_0 + A_1(1+z) + A_2(1+z)^2}{A_0 + A_1 + A_2} \right]^{\frac{D-1}{3}} \quad (25)$$

$$p = \left[-1 + \frac{A_1(1+z) + 2A_2(1+z)^2}{3\{A_0 + A_1(1+z) + 2A_2(1+z)^2\}} \right] \rho_0 \left[\frac{A_0 + A_1(1+z) + A_2(1+z)^2}{A_0 + A_1 + A_2} \right]^{\frac{D-1}{3}} \quad (26)$$

$$\phi = \phi_0 + \sqrt{\frac{(D-1)(D-2)}{6}} \int \sqrt{\frac{2A_2 + \frac{A_1}{1+z}}{A_0 + A_1(1+z) + A_2(1+z)^2}} dz \quad (27)$$

$$U = \left[1 - \frac{A_1(1+z) + 2A_2(1+z)^2}{6\{A_0 + A_1(1+z) + A_2(1+z)^2\}} \right] \rho_0 \left[\frac{A_0 + A_1(1+z) + A_2(1+z)^2}{A_0 + A_1 + A_2} \right]^{\frac{D-1}{3}} \quad (28)$$

We draw the variations of energy density ρ , pressure p , EoS parameter $\omega(z)$, Hubble parameter H , potential $U(\phi)$ and the scalar field ϕ with the variation in z in Figs. 22 - 27 respectively. Fig. 28 shows the variation of $U(\phi)$ with ϕ . We observe that ρ , H , ϕ and $U(\phi)$ decrease as z decreases. p increases as z decreases but keeps negative sign. ω first decreases up to certain value of z and then increases as z decreases. Also $U(\phi)$ increases as ϕ increases.

E. Model V: Efstathiou parametrization

Here, in Efstathiou parametrization model, the equation of state takes the form [42, 43] $\omega = \omega(z) = \omega_0 + \omega_1 \log(1+z)$, where again ω_0 and ω_1 are constants. This gives rise to the following terms

$$\rho = \rho_0(1+z)^{(D-1)(1+\omega_0)} e^{\frac{(D-1)\omega_1}{2} [\log(1+z)]^2} \quad (29)$$

$$p = [\omega_0 + \omega_1 \log(1+z)] \rho_0(1+z)^{(D-1)(1+\omega_0)} e^{\frac{(D-1)\omega_1}{2} [\log(1+z)]^2} \quad (30)$$

$$\phi = \phi_0 + \frac{\sqrt{2(D-1)(D-2)}}{3\omega_1} [1 + \omega_0 + \omega_1 \log(1+z)]^{\frac{3}{2}} \quad (31)$$

$$U = \frac{1}{2} [1 - \omega_0 - \omega_1 \log(1+z)] \rho_0(1+z)^{(D-1)(1+\omega_0)} e^{\frac{(D-1)\omega_1}{2} [\log(1+z)]^2} \quad (32)$$

We draw the variations of energy density ρ , pressure p , EoS parameter $\omega(z)$, Hubble parameter H , potential $U(\phi)$ and the scalar field ϕ with the variation in z in Figs. 29 - 34 respectively. Fig. 35 shows the variation of $U(\phi)$ with ϕ . We observe that ρ , H , and $U(\phi)$ first decrease up to certain value of z as z decreases and then sharply increase as z decreases. But p first decreases from positive level to negative level then slightly increases and then sharply decreases as z decreases but keeps the negative sign. ω decreases from positive level to negative level as z decreases. ϕ decreases as z decreases. Also $U(\phi)$ increases as ϕ increases.

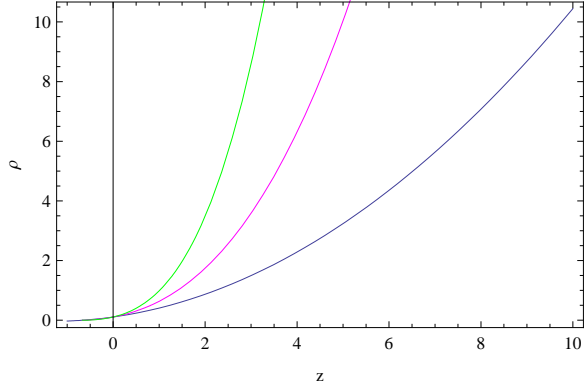


Fig.22

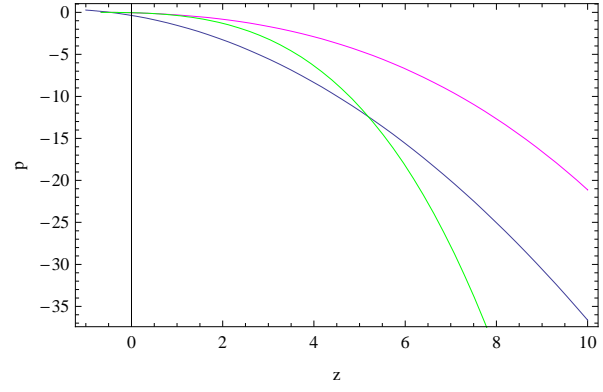


Fig.23

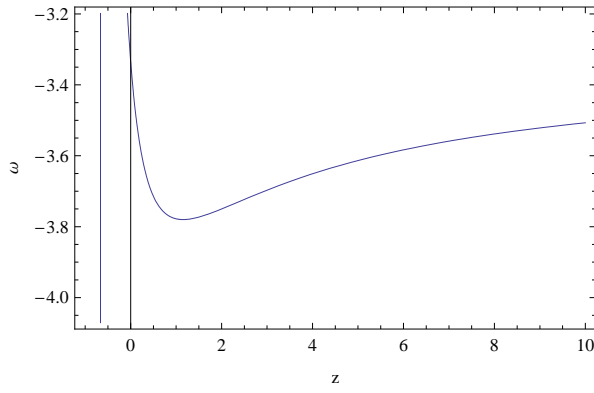


Fig.24

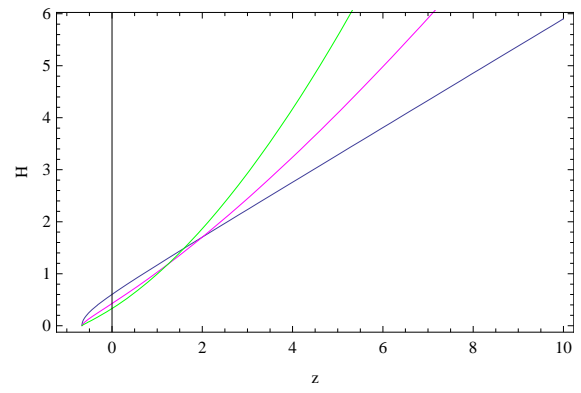


Fig.25

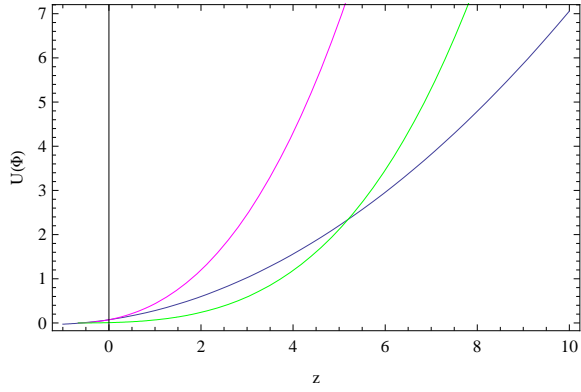


Fig.26

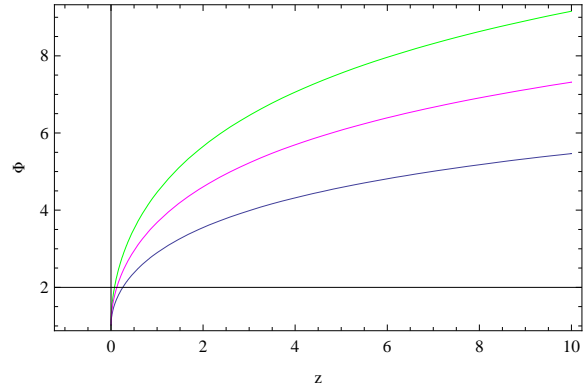


Fig.27

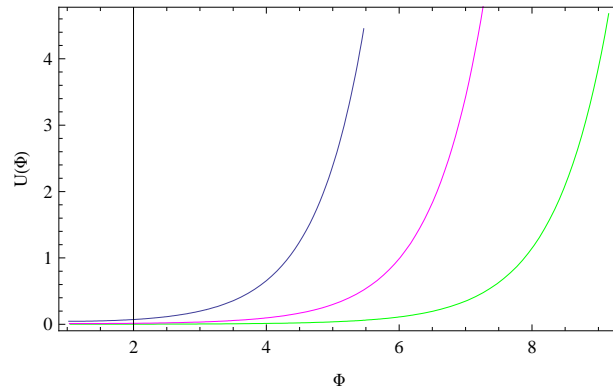


Fig.28

Figs. 22, 23, 24, 25, 26 and 27 show the variation of energy density ρ , pressure p , EoS parameter $\omega(z)$, Hubble parameter H , potential $U(\phi)$ and the scalar field ϕ with the variation in z for the **ASSS** parameterizations. Fig. 28 shows the variation of $U(\phi)$ with ϕ . Different colored paths are obtained for different values of D .

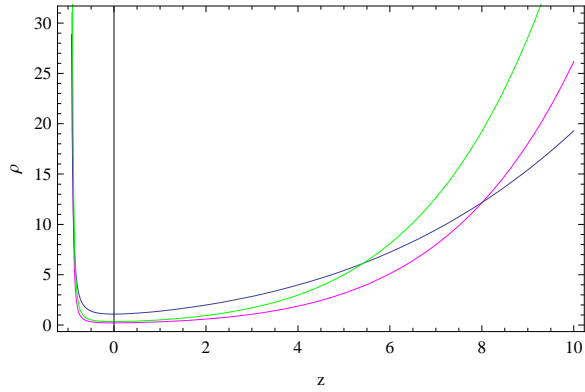


Fig.29

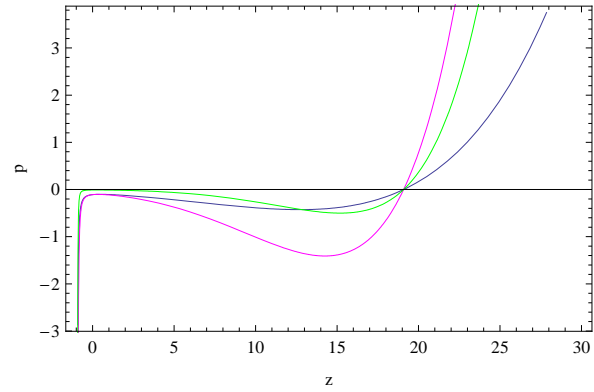


Fig.30

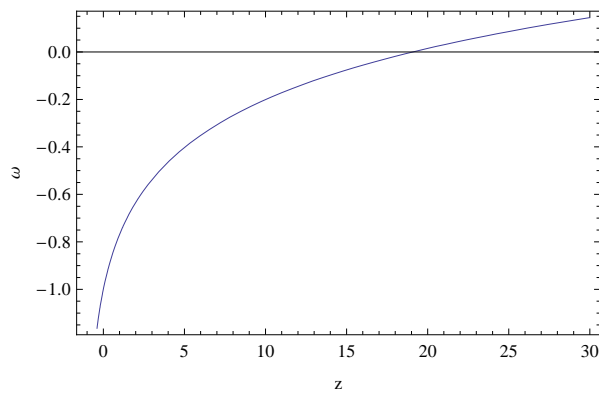


Fig.31

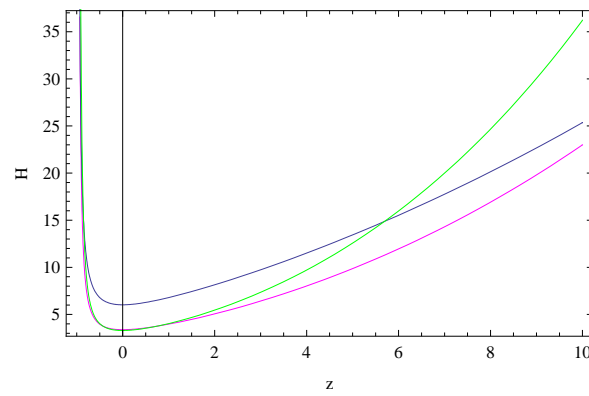


Fig.32

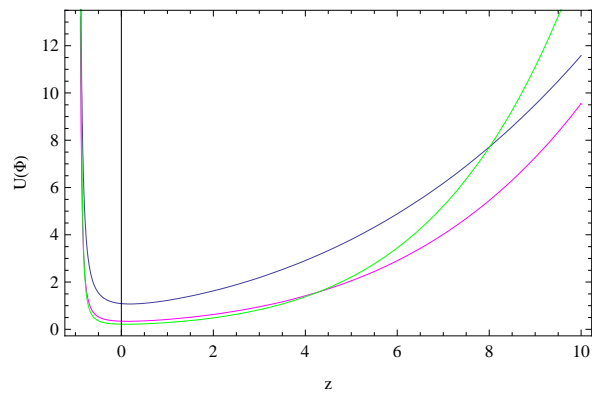


Fig.33

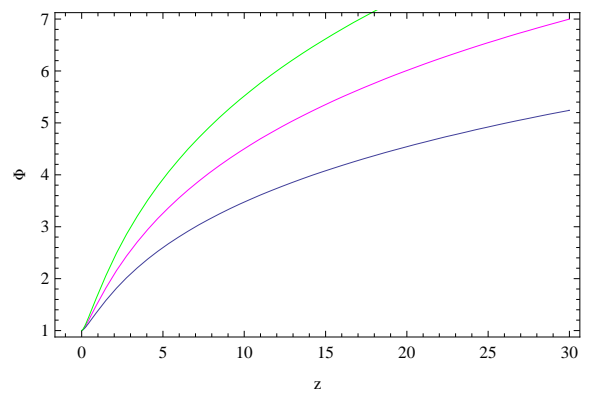


Fig.34

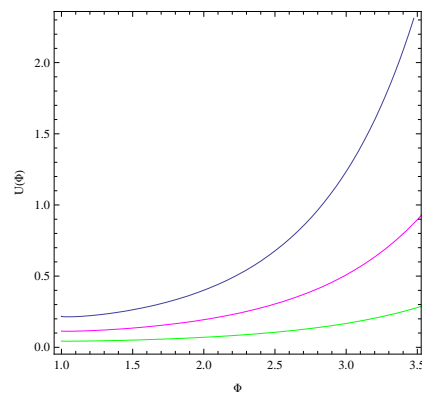


Fig.35

Figs. 29, 30, 31, 32, 33 and 34 show the variation of energy density ρ , pressure p , EoS parameter $\omega(z)$, Hubble parameter H , potential $U(\phi)$ and the scalar field ϕ with the variation in z for the **Efstathiou** parameterizations. Fig. 35 shows the variation of $U(\phi)$ with ϕ . Different colored paths are obtained for different values of D .

IV. ANALYSIS OF FUTURE SINGULARITIES

The future singularities can be classified in the following ways [44, 45]:

- Type I (Big Rip) : For $t \rightarrow t_s$, $a \rightarrow \infty$, $\rho \rightarrow \infty$ and $|p| \rightarrow \infty$
- Type II (Sudden) : For $t \rightarrow t_s$, $a \rightarrow a_s$, $\rho \rightarrow \rho_s$ and $|p| \rightarrow \infty$
- Type III : $t \rightarrow t_s$, $a \rightarrow a_s$, $\rho \rightarrow \infty$ and $|p| \rightarrow \infty$
- Type IV : For $t \rightarrow t_s$, $a \rightarrow a_s$, $\rho \rightarrow 0$ and $|p| \rightarrow 0$

where t_s , a_s and ρ_s are constants with $a_s \neq 0$.

The following table shows the restrictions on the parameters involved in the five parameterization models for the occurrence of the future singularities:

TABLE

| Singularity/Model | Linear | CPL | JBP | ASSS | Efstathiou |
|-------------------|-------------------------------|----------------|----------------|----------------------|----------------|
| Type I (Big Rip) | $1 + \omega_0 - \omega_1 < 0$ | $\omega_1 > 0$ | $\omega_1 > 0$ | No | $\omega_1 > 0$ |
| Type II (Sudden) | No | No | No | No | No |
| Type III | No | No | No | No | No |
| Type IV | No | No | No | $A_1^2 \geq 4A_0A_2$ | No |

V. BOUNCING UNIVERSE

The initial singularity in the cosmological models can be avoided by introducing the non-singular bouncing models. In these models, an universe undergoing a 'bounce' stage attains a minimum after a collapsing phase and then subsequently expands. During the collapse, the scale factor $a(t)$ decreases [$\dot{a}(t) < 0$] and during the expanding phase, it increases [$\dot{a}(t) > 0$]. At the bounce point, $t = t_b$, the minimal necessary condition (may not be sufficient) is $\dot{a}(t) = 0$ and $\ddot{a}(t) > 0$ for $t \in (t_b - c, t_b) \cup (t_b, t_b + c)$ for small $c > 0$. For a non-singular bounce $a(t_b) \neq 0$.

In the current study, the bouncing universe can be viewed in different parameterizing models from the figures 36-45, where the evolution of the scale factor $a(t)$ and the EoS parameter ω are shown with respect to time t for each model. For the bouncing phase, the scale factor first decreases and then increases in order that the universe enters into the hot Big Bang era immediately after the bounce. The nature of the equation of state parameters have been presented in the figures. The figures clearly show bouncing solutions for Linear, CPL, JBP, ASSS and Efstathiou models with a minimal non-zero scale factor $a(t)$.

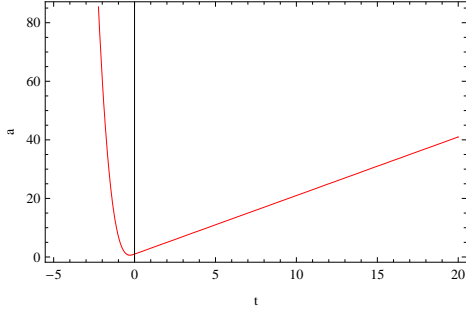


Fig.36

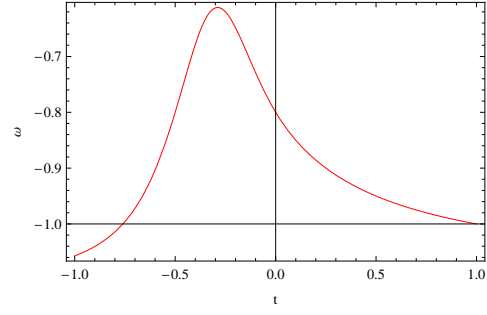


Fig.37

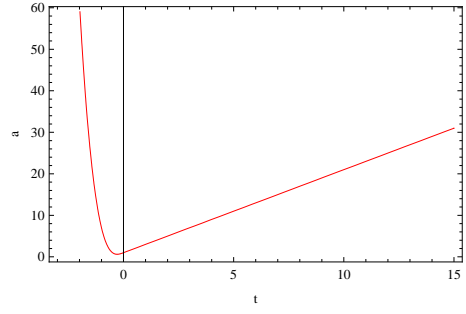


Fig.38

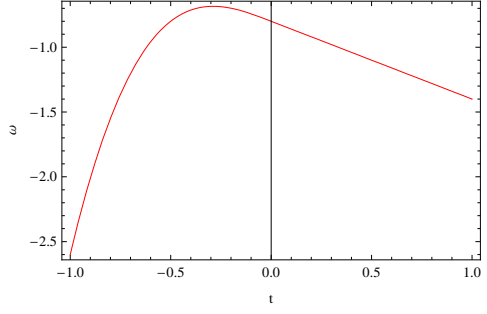


Fig.39

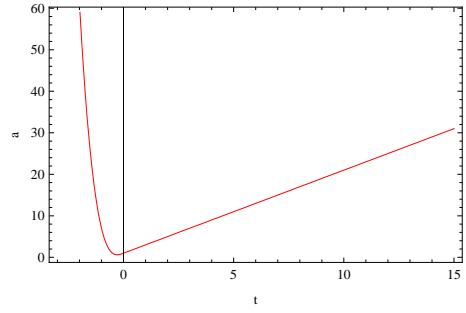


Fig.40

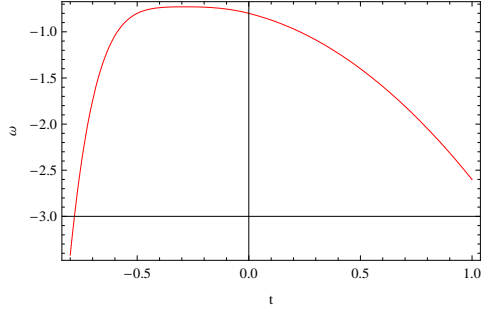


Fig.41

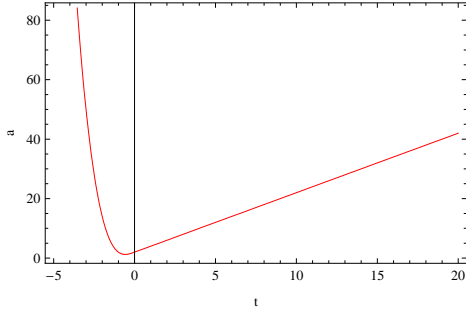


Fig.42

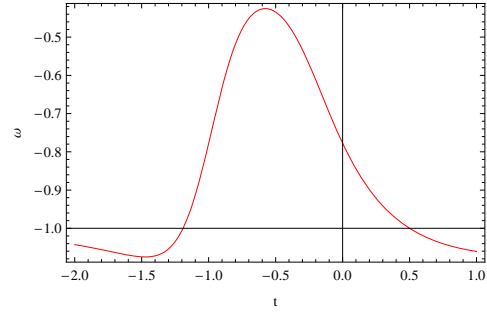


Fig.43

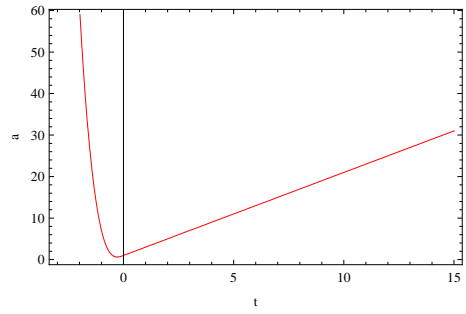


Fig.44

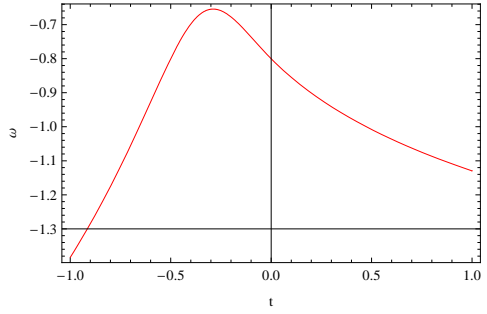


Fig.45

Figs. 36-37 (Linear), 38-39 (CPL), 40-41 (JBP), 42-43 (ASSS) and 44-45 (Efstathiou) show the variation of scale factor $a(t)$ (left) and EoS parameter ω (right) with the variation in cosmic time t for the different parameterization models.

VI. DISCUSSION

In this work, we have considered the D-dimensional flat FRW model of the Universe in the background of some well known parametrization of dark energy models like linear, CPL, JBP, ASSS and Efstathiou. By considering the scalar field model as these parametrizations of dark energy, we found the energy density, pressure, scalar field and corresponding potential in terms of the redshift z . In model I (linear), we have drawn the variations of energy density ρ , pressure p , EoS parameter $\omega(z)$, Hubble parameter H , potential $U(\phi)$ and the scalar field ϕ with the variation in z in Figs. 1 - 6 respectively. Fig. 7 shows the variation of $U(\phi)$ with ϕ . We have seen that ρ , H and ϕ decrease as z decreases. p and ω decrease from positive level to negative level as z decreases. $U(\phi)$ first increases up to certain value of z and then decreases as z decreases. Also $U(\phi)$ decreases as ϕ increases.

In model II (CPL), we have drawn the variations of energy density ρ , pressure p , EoS parameter $\omega(z)$, Hubble parameter H , potential $U(\phi)$ and the scalar field ϕ with the variation in z in Figs. 8 - 13 respectively. Fig. 14 shows the variation of $U(\phi)$ with ϕ . We have seen that ρ , H , and $U(\phi)$ first decrease up to $z = 0$ as z decreases and then sharply increase as z decreases. But p first increases up to $z = 0$ as z decreases and then sharply decreases as z decreases but keeps the negative level. ω decrease as z decreases and always keeps negative sign. ϕ increases as z decreases. Also $U(\phi)$ decreases as ϕ increases.

In model III (JBP), we have drawn the variations of energy density ρ , pressure p , EoS parameter $\omega(z)$, Hubble parameter H , potential $U(\phi)$ and the scalar field ϕ with the variation in z in Figs. 15 - 20 respectively. Fig. 21 shows the variation of $U(\phi)$ with ϕ . We have seen that ρ , H , and $U(\phi)$ first decrease up to $z = 0$ as z decreases and then sharply increase as z decreases. But p first increases up to $z = 0$ as z decreases and then sharply decreases as z decreases but keeps the negative level. ω first increases up to certain value of z and then sharply decreases but keeps negative sign. ϕ decreases as z decreases. Also $U(\phi)$ increases as ϕ increases.

In model IV (ASSS), we have drawn the variations of energy density ρ , pressure p , EoS parameter $\omega(z)$, Hubble parameter H , potential $U(\phi)$ and the scalar field ϕ with the variation in z in Figs. 22 - 27 respectively. Fig. 28 shows the variation of $U(\phi)$ with ϕ . We have seen that ρ , H , ϕ and $U(\phi)$ decrease as z decreases. p increases as z decreases but keeps negative sign. ω first decreases up to certain value of z and then increases as z decreases. Also $U(\phi)$ increases as ϕ increases.

In model V (Efstathiou), we have drawn the variations of energy density ρ , pressure p , EoS parameter $\omega(z)$, Hubble parameter H , potential $U(\phi)$ and the scalar field ϕ with the variation in z in Figs. 29 - 34 respectively. Fig. 35 shows the variation of $U(\phi)$ with ϕ . We have seen that ρ , H , and $U(\phi)$ first decrease up to certain value of z as z decreases and then sharply increase as z decreases. But p first decreases from positive level to negative level then slightly increases and then sharply decreases as z decreases but keeps the negative sign. ω decreases from positive level to negative level as z decreases. ϕ decreases as z decreases. Also $U(\phi)$ increases as ϕ increases.

Also the present work is designed to investigate the possibilities of finite time future singularities i.e., types I (big rip), II (sudden), III and IV singularities. From the table, we observe that for linear parametrization model, the type I (big rip) singularity occurs provided $1 + \omega_0 - \omega_1 < 0$, but types II-IV singularities cannot occur. For CPL parametrization model, the type I (big rip) singularity occurs provided $\omega_1 > 0$, but types II-IV singularities cannot occur. For JBP parametrization model, the type I (big rip) singularity occurs provided $\omega_1 > 0$, but types II-IV singularities cannot occur. For ASSS parametrization model, the types I-III singularities cannot occur, only type IV singularity occurs provided $A_1^2 \geq 4A_0A_2$. For Efstathiou parametrization model, the type I (big rip) singularity occurs provided $\omega_1 > 0$, but types II-IV singularities cannot occur.

Conflicts of Interest: The authors declare that there is no conflict of interest regarding the publication of this paper.

Acknowledgement: The authors are thankful to IUCAA, Pune, for their warm hospitality where most of the work has been done during a visit under the Associateship Programme.

-
- [1] A. Borde and A. Vilenkin, *Phys.Rev.Lett.* **72**, 3305, (1994).
- [2] M. Novello and S. E. Perez Bergliaffa, *Phys.Rept.* **463**, 127, (2008).
- [3] J.-L. Lehners, *Class.Quant.Grav.* **28**, 204004, (2011).
- [4] Y. F. Cai and E. N. Saridakis, *J.Cosmol.* **17**, 7238, (2011).
- [5] J. Khoury, B. A. Ovrut and J. Stokes, *JHEP* **08**, 015, (2012).
- [6] Y. F. Cai, D. A. Easson and R. Brandenberger, *JCAP* **08**, 020, (2012).
- [7] M. Koehn, J.-L. Lehners and B. A. Ovrut, *Phys.Rev.D* **90**, 025005 (2014).
- [8] Y. F. Cai and E. Wilson-Ewing, *JCAP* **08**, 1403, (2014).
- [9] S. D. Odintsov and V. K. Oikonomou, *Phys.Rev.D* **91**, 064036 (2015).
- [10] S. D. Odintsov and V. K. Oikonomou, *Phys.Rev.D* **94**, 064022 (2016).
- [11] Y. F. Cai et al. *JHEP* **0710**, 071 (2007).
- [12] A. G. Riess et al., [Supernova Search Team Collaboration], *Astron.J.* **116**, 1009 (1998).
- [13] A. G. Riess et al., [Supernova Search Team Collaboration], *Astrophys.J.* **607**, 665 (2004).
- [14] S. Perlmutter et al., [Supernova Cosmology Project Collaboration], *Nature (London)* **391**, 51 (1998).
- [15] S. Perlmutter et al., [Supernova Cosmology Project Collaboration], *Astrophys.J.Suppl.* **517**, 565 (1999).
- [16] P. M. Garnavich et al., (Hi-Z Supernova Team Collaboration), *Astrophys.J.* **493**, L53 (1998).
- [17] C. L. Bennett et al., *Astrophys.J.Suppl.* **148**, 1 (2003).
- [18] D. N. Spergel et al., [WMAP Collaboration], *Astrophys.J.Suppl.* **148**, 175 (2003).
- [19] L. Verde et al., *Mon.Not.R.Astron.Soc.* **335**, 432 (2002).
- [20] E. Hawkins et al., *Mon.Not.R.Astron.Soc.* **346**, 78 (2003).
- [21] K. Abazajian et al., [SDSS Collaboration], *Phys.Rev.D* **69**, 103501 (2004).
- [22] B. Ratra, P. J. E. Peebles, *Phys.Rev.D* **37**, 3406 (1988).
- [23] I. Zlatev, L. Wang and P. J. Steinhardt, *Phys.Rev.Lett.* **82**, 896 (1999).
- [24] **A. Yu. Kamenshchik, U. Moschella and V. Pasquier, *Phys. Lett. B* **511**, 265 (2001).**
- [25] F. C. Santos, M. L. Bedran and V. Soares, *Phys.Lett.B* **646**, 215 (2007).
- [26] C. Armendariz-Picon, V. Mukhanov and P. J. Steinhardt, *Phys.Rev.Lett.* **85**, 4438 (2000).
- [27] L. Randal and R. Sundrum, *Phys.Rev.Lett.* **83**, 3370 (1999).
- [28] L. Randal and R. Sundrum, *Phys.Rev.Lett.* **83**, 4690 (1999).
- [29] C. Deffayet, G. Dvali and G. Gabadadze, *Phys.Rev.D* **65**, 044023 (2002).

- [30] V. Sahni and Y. Shtanov, *JCAP*, **0311**, 014 (2003).
- [31] B. Boisseau, G. Esposito-Farese, D. Polarski and A. A. Starobinsky, *Phys.Rev.Lett.* **85**, 2236 (2000).
- [32] J. M. Cline, S. Jeon and G. D. Moore, *Phys.Rev.D* **70**, 043543 (2004).
- [33] **V. Sahni and A. A. Starobinsky, *IJMPD* **15**, 2105 (2006).**
- [34] S. Sadatian, *Int.J.Theor.Phys.* **53**, 675 (2014).
- [35] K. Bamba, S. Capozziello, S. Nojiri and S. D. Odintsov, *Astrophys.Space Sci.* **342**, 155 (2012).
- [36] Cooray, A. R., Huterer, D. :- *Astrophys. J.* **513** L95(1999).
- [37] Chevallier, M., Polarski, D. :- *Int. J. Mod. Phys. D* **10** 213(2001).
- [38] Linder, E. V. :- *Phys. Rev. Lett.* **90** 091301(2003).
- [39] Jassal, H. K., Bagla, J. S., Padmanabhan, T. :- *MNRAS* **356** L11(2005).
- [40] U. Alam, V. Sahni, T. D. Saini and A. A. Starobinsky, *Mon. Not. R. Astron. Soc.* **354** 275 (2004).
- [41] U. Alam, V. Sahni and A. A. Starobinsky, *JCAP* **0406** 008 (2004).
- [42] G. Efstathiou, *Mon. Not. R. Astron. Soc.* **310** 842 (1999).
- [43] R. Silva, J. S. Alcaniz and J. A. S. Lima, *Int. J. Mod. Phys. D* **16** 469 (2007).
- [44] B. McInnes, *JHEP* **0208**, 029 (2002).
- [45] S. Nojiri, S. D. Odintsov and S. Tsujikawa, *Phys.Rev.D* **71**, 063004 (2005).